SJST
sjst.scst.edu.ly
Surman Journal for Science and Technology
ISSN: Online (2790-5721) - Print (2790-5713)
مجلة صرمان للعلوم والتقنية
Vol6, No.2, Jun. – Dec. 2024
Pages: 150 ~ 167

Generating Motion by Optimizing the Rowat and Silverstone of Neural Oscillator for Defining Human Gait Patterns

Esra Abdalftah[1], Abdalftah Elbori[2]

[1]Mathematical Department, Faculty of Science Azzaytuna University, Tarhuna-Libya

[2]Department of Mathematics Faculty of Science Azzaytuna University, Tarhuna-Libya

[1]asraalarbi3@gmail.com
[2]abdalftah81@yaahoo.com

Abstract

This study discusses the effect of the Rowat and Silverstone of Neural Oscillator for Defining Human Gait Patterns by using both the Genetic Algorithm and hybrid function. By omitting pulse generators in the Rowat and Silverstone of Neural Oscillator, because of that it changes to a new type of Central Patterns Generator. By optimizing a new type and compare with the real data that we get from Tema Motion software. This paper will show that it is possible to produce rhythmic patterns like the rhythmic patterns derived from real data without any sensor feedback. This study will also be concerned with the most effective parameters of the Rowat and Silverstone Neural Oscillator

Keywords: *The Rowat and Silverstone, Mathematical Modeling of One leg, stability analysis, Optimizing, The Rowat and Silverstone, Hybrid Function.*

INTROCUCTION

A neural oscillator is formed by two neurons with inhibitive connections between them. The responses of two neurons of a neural oscillator suppress each other in such way one of them is extensor neuron and the other is flexor neuron. neural oscillators generally refer to rhythmic activity patterns observed in neural networks. These patterns are fundamental in various brain functions, including sensory processing, motor control, and cognitive processes. Researchers like Rowat and Silverstone might have contributed to this field through studies on how neural oscillations emerge, their mechanisms, or their role in brain function. Central Pattern Generators (CPGs) are found in the spine of both vertebrate and invertebrate animals and burst signal from the brainstem induces a periodic activity in the CPG [1], [2].

To begin with, CPGs are neural networks located in the spinal cord of vertebrate as well as invertebrate animals. These CPGs are designed to exclusively supply synchronized rhythmic pattern activities, viz., leg movement in the course of walking, respiration, or chewing [3] and [4]. One of the captivating characteristics of CPGs lies in their capacity to generate rhythmic signals over and above any rhythmic contribution from higher control centers or sensory response. In addition, CPGs are vigorous, versatile, and effortlessly adjustable. These compelling attributes render CPGs expedient for mobility control of robots with multiple joints, degrees of freedom (DOF), and even for kinematically redundant robots. Research into bio-robotics has recently gained unprecedented momentum. The interest in the application of robots to enhance traditional mechatronics systems or to attend to particular issues related to biology has brought bio-robotics back to life, but with a different spirit [1] and [2]. The focus now is on how, in robotics, CPGs can be effectively manipulated to administer cadenced movements

related to crawling, flying, and swimming, and not only legged walking (for more details, see [3], [4] and [5]).

A plethora of studies on CPGs have introduced fascinating results. Some of these studies have indicated that CPGs can in fact control some functions in the human body, viz., breathing and digestion [3], [5] and [6]. Other studies, based on the suppressive or stimulatory connection between the extensor neuron and the flexor neuron [7], [8] and [9], have revealed the potential of modelling a variety of physical structures of the limbs and arms of robots (see [10], [11], [12], [13] and [14]) by copying the control systems of robots. In the realm of robotics, numerous mathematical and physical models have been developed to mimic the movements of living creatures and reproduce rhythmic patterns akin to those observed in real biological systems. The Rowat-Selverston model primarily revolves around understanding the dynamics of rhythmic neural activity, such as the visual activity patterns in CPGs that control rhythmic movements in animals. The Rowat-Selverston model is designed to provide insights into the electrical properties and interactions between neurons within these neural circuits.

Finally, some CPG configurations have been utilized to control biped locomotion in humanoid robots (see, [15], [16], [17], [18] and [19]).

This paper figures out the effect of optimizing The Rowat-Selverston neural osculators, on the performance of one-leg movement of humans. First section in this study will discuss the simple kinematics systems of one leg with three degrees of Freedoms (3DOFs). The Second section, it discusses The Rowat and Silverstone of Neural Oscillator Model and change it to CPGs Model. Third section, we will look the stability analysis of the model. Fourth section will explain the way to get real data that will be used for comparison. Final section, it undertakes to optimize The Rowat-Selverston neural osculators and compare with real data with some new cost functions.

KINEMATIC ANALYSIS AND MODELLING OF BIPED LOCOMOTION SYSTEMS

Using actual data is likely the simplest and most direct approach to generate a trajectory of accelerated motion induced by Central Pattern Generators (CPG) or neural oscillators for bipedal locomotion. To understand the kinematic characteristics during walking, we initially explore the principles of bipedal kinematics in the sagittal plane, outlining the fundamental kinematic rules for robotic bipedal locomotion involving two or three degrees of freedom. [20] and [21]. We will compare the forward motion trajectory derived from actual data with that generated by CPGs. Figure 1 demonstrates how CPGs can be fine-tuned to create rhythmic patterns in the hip, knee, and ankle angles for one leg of a human when the lower body is horizontal. It's important to note that the outcomes depend on the method used to analyze CPGs.

sjst.scst.edu.ly
Surman Journal for Science and Technology
ISSN: Online (2790-5721) - Print (2790-5713)
مجلة صرمان للعلوم والتقنية
Vol6, No.2, Jun. – Dec. 2024
Pages: 150 ~ 167

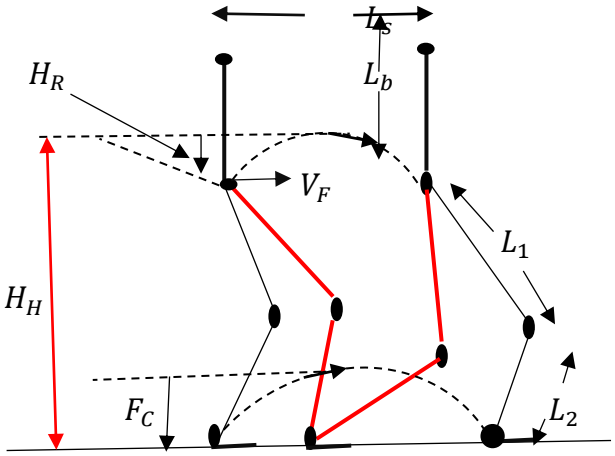

Figure 1: The Planar biped model when the lower body is parallel to the ground

A closer look into the kinematics of the hip, knee, and ankle angles in the swing phase reveals the following basic kinematics equations:
The first coordinate (x_1, y_1) yields

$$x_1 = x_d + L_1 cos\theta_1 \quad \text{and} \quad y_1 = y_d + L_1 sin\theta_1.$$

The second coordinate (x_2, y_2) reveals that

$$x_2 = x_d + L_1 cos\theta_1 + L_2 cos\theta_2 \quad \text{and} \quad y_2 = y_d + L_1 sin\theta_1 + L_2 sin\theta_2,$$

and the third coordinate (x_3, y_3) translates into

$$x_3 = x_2 + L_3 cos\theta_3 \quad \text{and} \quad y_3 = y_2 + L_3 sin\theta_3,$$

where x_d is the proceeding displacement (i.e., the distance during locomotion) and y_d stands for the positive direction of the hip height at each step. L_1, L_2, and L_3 represent three lengths: from the hip joint to the knee joint, from the knee joint to the ankle joint, and from the ankle joint to the end effector, respectively. The angles, θ_1, θ_2 and θ_3, which represent the hip, knee, and ankle angles, respectively, will acquire their rhythmic patterns from CPGs. With regard to y_d , It was presumed to be zero when the lower body was parallel to the ground. However, in this study, the researchers immobilized the hip joint, even though it was not immobilized during data collection.

THE ROWAT AND SELVERSTON OF NEURAL OSCILLATOR MODEL TO CPGS MODEL:

Biological neurons with several ionic channels are complex, hence difficult to model. Rowat and Silverstone (1993) present a simple model of a neuron for which two groups of currents are identified: a fast current and a slow current, each defined by a first order differential equation. Fast current is defined by Eq. 1 and slow current by Eq. 2.

$$\tau_m \left(\frac{dV}{dt}\right) = -F(V, \sigma_f) - q + I_{inj} \qquad (1)$$

$$\tau_s \left(\frac{dq}{dt}\right) = -q + \sigma_s V \qquad (2)$$

where

$$F(V, \sigma_f) = V - A_f tan\, h\left(\frac{\sigma_f V}{A_f}\right)$$

Where τ_m and τ_s are the time constant of the neuron and the time constant of slow currents activation respectively. Where $\tau_m < \tau_s$, I_{inj} is the injected current, V the cellular membrane voltage, and q the slow current. $F(V, \sigma_f)$ is a non-linear current voltage for the fast current, and A_f adjusts the width and without affecting the degree of the N-shape.

The results obtained from the model were compared to the actual/true results, and it was found that the injected current caused errors, which hindered the comparison. As a result, the injected current I_{inj} was removed/deleted. This led to the model shifting from a neural to a central pattern generator (CPG).

$$\tau_m \left(\frac{dV}{dt}\right) = -F(V, \sigma_f) - q \qquad (3)$$

$$\tau_s \left(\frac{dq}{dt}\right) = -q + \sigma_s V \qquad (4)$$

where

$$F(V, \sigma_f) = V - A_f \tan h\left(\frac{\sigma_f V}{A_f}\right)$$

STABILITY ANALYSIS

In this part, the stability analysis for each type of coupling given in the previous section will be discussed. We consider one neural as:

$$\left.\begin{aligned} \tau_m \left(\frac{dV}{dt}\right) &= -F(V, \sigma_f) - q \\ \tau_s \left(\frac{dq}{dt}\right) &= -q + \sigma_s V \\ F(V, \sigma_f) &= V - A_f \tanh\left(\frac{\sigma_f V}{A_f}\right) \end{aligned}\right\} \qquad (5)$$

It is enough to find to analysis one to know the stabile region:

We know that :

$$\tanh^{-1}(z) = \frac{1}{2} Log\left(\frac{1+z}{1-z}\right), |z| < 1 \quad also\ tanh(z) = \frac{e^z - e^{-z}}{e^z + e^{-z}}$$

$$Logz = Ln(r) + i(\theta + 2n\pi) \quad , r > 0\,, \alpha < \theta < \alpha + 2\pi$$

To find the equilibrium points of the given system (5), we need to find values of V and q such that both equations are satisfied:

$$\tau_m \left(\frac{dV}{dt}\right) = -F(V, \sigma_f) - q$$

$$\tau_s \left(\frac{dq}{dt}\right) = -q + \sigma_s V$$

Let's first focus on the first equation:

$$\tau_m \left(\frac{dV}{dt}\right) = -F(V, \sigma_f) - q$$

Rearranging the equation:

$$\tau_m \left(\frac{dV}{dt}\right) = -q - F(V, \sigma_f)$$

Now, let's look at the second equation:

$$\tau_s\left(\frac{dq}{dt}\right) = -q + \sigma_s V$$

Rearranging this equation:

$$\tau_s\left(\frac{dq}{dt}\right) + q = \sigma_s V$$

Now, we want to find values of V and q such that both equations are satisfied simultaneously. This means that at the equilibrium points, both left-hand sides (LHS) and right-hand sides (RHS) of these equations must be equal. Therefore, we have:

Equilibrium for the first equation:

$$\tau_m\left(\frac{dV}{dt}\right) = -q - F(V, \sigma_f)$$

At equilibrium, $\frac{dV}{dt} = 0$, so we get:

$$0 = -q - F(V, \sigma_f)$$

Equilibrium for the second equation:

$$\tau_s\left(\frac{dq}{dt}\right) + q = \sigma_s V$$

At equilibrium, $\frac{dq}{dt} = 0$, so we get:

$$q = \sigma_s V$$

Now, we have two equations:

$$0 = -q - F(V, \sigma_f)$$
$$q = \sigma_s V$$

We can substitute the second equation into the first to find the equilibrium points:

$$0 = -\sigma_s V - F(V, \sigma_f) \Rightarrow 0 = -\sigma_s V - \left(V - A_f \tanh\left(\frac{\sigma_f V}{A_f}\right)\right)$$

Now, we need to solve this equation for V. The specific form of $F(V, \sigma_f)$ is not provided, so the equilibrium points will depend on the function $F(V, \sigma_f)$. You would need to know the details of $F(V, \sigma_f)$ to find the exact equilibrium points. Essentially, you'll need to solve this equation for V with the specific form of $F(V, \sigma_f)$. Keep in mind that this is a nonlinear equation, and the solutions may not have a simple closed-form expression. You may need to use numerical methods or software to find the equilibrium points numerically.

Firstly: we k need to find the equilibrium points as the following the steps

$$\left(\frac{dV}{dt}\right) = \frac{1}{\tau_m}\left(-V + A_f \tanh\left(\frac{\sigma_f V}{A_f}\right) - q\right) = 0$$
$$\left(\frac{dq}{dt}\right) = \frac{1}{\tau_s}(-q + \sigma_s V) = 0$$

The first the equilibrium point is the origin point when we assume that $I_{inj} = 0$. In this case we will have CPG instead of neural.

OPTAINING REAL DATA AND OPTIMIZATION

We used a high-speed camera to capture the movement of the leg, as depicted in Figure 2. This recording provided us with actual data on how the leg moves under various conditions. Analyzing this data helped us assess the validity of our findings. Additionally, we compared this real-world data with results generated by Central Pattern Generators (CPG) to evaluate the accuracy of these results and how closely they replicate natural leg motion.

Figure. 2: Video-recorded data and high-speed camera

The researchers utilized the Tema Motion software to analyze video-recorded real data. The outcomes from using Tema Motion to determine the hip and knee angles are depicted in Figure 3.

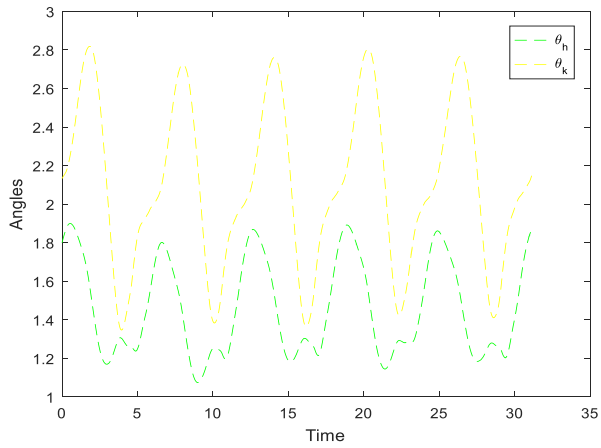

Figure 3: Angles of the hip and knee that are collected by real data

Our objective is to contrast actual data with enhanced neural oscillators that generate movement patterns in a single leg with two degrees of freedom, mimicking natural leg motion. each pattern generator generates joint angle patterns, and we employed a genetic algorithm to derive motion in the x direction and identify the optimal parameter set for this motion. to achieve this, we utilized the following objective function :

$$J = \sum_{k=1}^{m} \left(\left(\theta_1(k) - \theta_h(k)\right)^2 + \left(\theta_2(k) - \theta_k(k)\right)^2 \right)$$

Expressing the equation mentioned earlier in words shows that θ_1 and θ_2 represent the outputs of the previously defined Central Pattern Generators (CPGs). where θ_h and θ_k are the angles

of hip and knee of the real data respectively and that m is the total number of step times. The conclusive goal here is to minimize differences between the outputs of the CPGs and the real data for the angles of the hip and the knee in the region captured by stability analysis. In addition, the equation above unfolds two constraints, namely $0 \leq \theta_1,\ \theta_2 \leq \pi$. In this study, a hybrid function was employed post-Genetic Algorithm (GA) termination to enhance the fitness function value during optimization. This hybrid function is notable because it starts from the GA's final point, which can be specified within the hybrid function's settings. The optimization' results are showing in the following Tables 1, 2, 3, 4 and 5

Tables 1: Uncoupled two neural networks in bounded in 31.13 seconds (N_in_pop=45)

Start at initial points	Parameters value $\{\sigma_{s1,}\ \sigma_{f1}, \tau_{s1}, \tau_{m1}, A_{f1}, I_{inj1}, \sigma_{s2,}\ \sigma_{f2}, \tau_{s2},$ $\tau_{m2}, A_{f2}, I_{inj2}, s_1, s_2, s_3, s_4\}$	J	x_b	Cross over
1.0809 2.1563 0.3697 0.3483 0.0052 0.2652 1.2747 0.2544 0.0630 18.7184 1.8607 1.8131 0.5051 2.0399	1.0811 2.1565 0.3697 0.3484 10.0057 0.2654 1.2748 0.2544 0.0631 18.7190 1.8609 1.8128 0.5054 2.0405	34.5354	0.8890	0.2
	1.0812 2.1565 0.3697 0.3487 10.0039 0.2655 1.2749 0.2544 0.0631 18.7183 1.8611 1.8136 0.5067 2.0429	34.5349	0.8969	0.4
	1.0813 2.1567 0.3698 0.3486 10.0036 0.2656 1.2750 0.2545 0.0632 18.7179 1.8620 1.8140 0.5069 2.0436	34.5334	0.8828	0.6
	0.3360 1.3503 0.2851 0.0881 11.5815 0.2671 1.2745 0.2226 0.0564 21.2114 0.5871 1.8128 0.5154 2.0507	33.9190	0.9036	0.8
	0.3360 1.3503 0.2851 0.0881 11.5815 0.2671 1.2745 0.2226 0.0564 21.2114 0.5871 1.8128 0.5154 2.0507	34.1615	0.9007	1.0

The results of Table 1 are showing by the following Figures

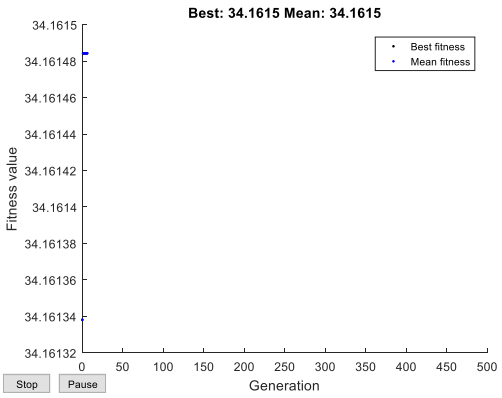

Figure 4: The optimization results are corresponding to the initial conditions $V(0) = 1$ and $q(0) = 1$, with crossover 1.0.

Surman Journal for Science and Technology
ISSN: Online (2790-5721) - Print (2790-5713)
sjst.scst.edu.ly
مجلة صرمان للعلوم والتقنية
Vol6, No.2, Jun. – Dec. 2024
Pages: 150 ~ 167

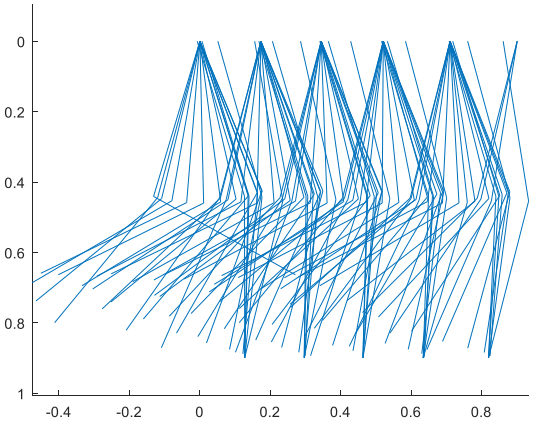

Figure 5 : One leg animation Uncoupled two CPGs: This animation corresponds to the values: $\sigma_{s1} = 0.3360$, $\sigma_{f1} = 1.3503$, $\tau_{s1} = 0.2851, \tau_{m1} = 0.0881,$ $A_{f1} = 11.5815,$ $\sigma_{s2} = 0.2671,$ $\sigma_{f2} = 1.2745$, $\tau_{s2} = 0.2226, \tau_{m2} = 0.0564, A_{f2} = 21.2114$, $s_1 = 0.5871, s_2 = 1.8128, s_3 = 0.5154, s_4 = 2.0507$,. This solution corresponds to the same values in Figure4

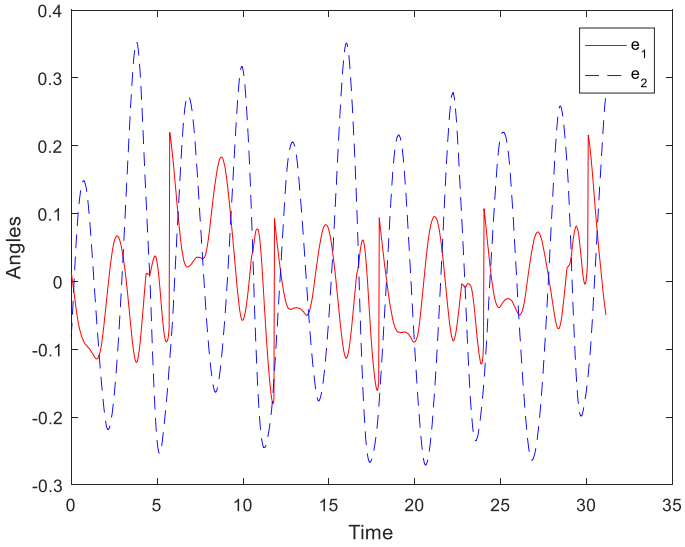

Figure 6: The Error between outputs of CPGs and Real data

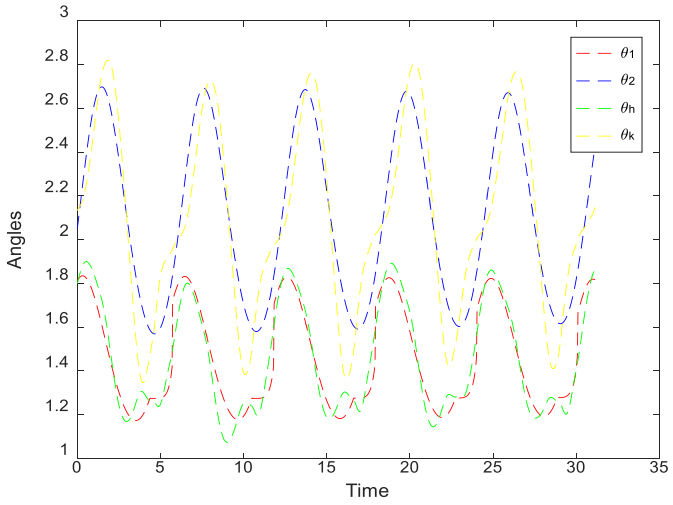

Figure 7: Angles of the real data and output of CPGs

Tables 2: Uncoupled two neural networks in bounded in 31.13 seconds (N_in_pop=60)

Start at initial points	Parameters value $\{\sigma_{s1}, \sigma_{f1}, \tau_{s1}, \tau_{m1}, A_{f1}, I_{inj1}, \sigma_{s2}, \sigma_{f2}, \tau_{s2}, \tau_{m2}, A_{f2}, I_{inj2}, s_1, s_2, s_3, s_4\}$	J	x_b	Cross over
0.3360 1.3503 0.2851 0.0881 11.5815 0.2671 1.2745 0.2226 0.0564 21.2114 0.5871 1.8128 0.5154 2.0507	0.2219 1.2316 0.2907 0.0592 12.2378 0.2639 1.2702 0.2070 0.0522 22.7822 0.3892 1.8198 0.5116 2.0518	33.6660	0.9151	0.2
	0.2222 1.2319 0.2908 0.0593 12.2399 0.2640 1.2703 0.2073 0.0523 22.7821 0.3906 1.8208 0.5122 2.0527	33.6770	0.8856	0.4
	0.2223 1.2320 0.2911 0.0593 12.2561 0.2640 1.2703 0.2073 0.0523 22.7623 0.3904 1.8212 0.5123 2.0529	33.6471	0.8924	0.6
	0.2231 1.2328 0.2895 0.0592 12.2932 0.2553 1.2615 0.2082 0.0508 22.7847 0.3906 1.8158 0.4940 2.0482	33.6915	0.8810	0.8
	0.2196 1.2289 0.2855 0.0576 12.4650 0.1568 1.1609 0.2154 0.0322 24.7881 0.3839 1.8137 0.2993 2.0234	33.8839	0.8832	1.0

Surman Journal for Science and Technology
ISSN: Online (2790-5721) - Print (2790-5713)
sjst.scst.edu.ly
مجلة صرمان للعلوم والتقنية
Vol6, No.2, Jun. – Dec. 2024
Pages: 150 ~ 167

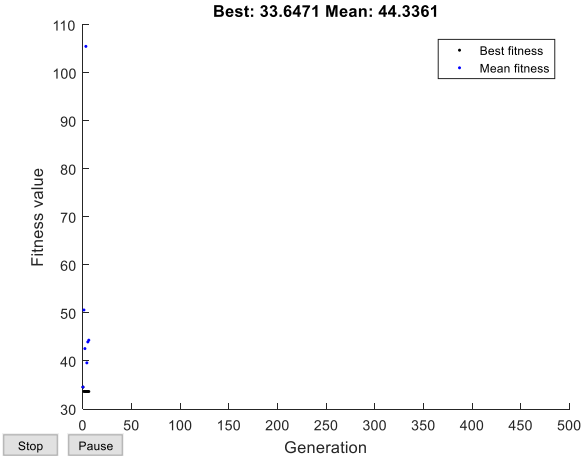

Figure 8: The optimization results are corresponding to the initial conditions $V(0) = 1$ and $q(0) = 1$, with crossover 0.6.

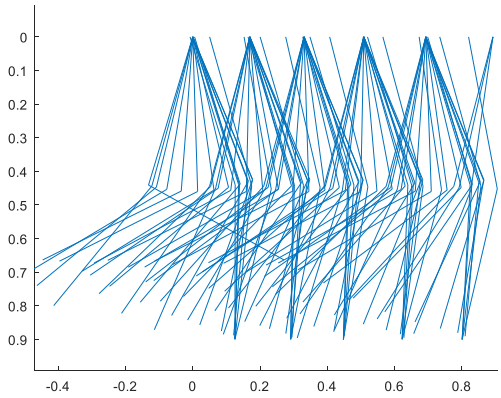

Figure 9 : One leg animation Uncoupled two CPGs: This animation corresponds to the values: $\sigma_{s1} = 0.2223,\ \sigma_{f1} = 1.2320,\ \tau_{s1} = 0.2911\ , \tau_{m1} =\ 0.0593,\ \ A_{f1} = 12.2561,\ \ \sigma_{s2} = 0.2640\ ,\ \sigma_{f2} = 1.2703, \tau_{s2} = 0.2073,\ \ \tau_{m2} = 0.0523\ , A_{f2} = 22.7623, \mathrm{s}_1 = 0.3904\ , \mathrm{s}_2 = 1.8212, \mathrm{s}_3 =\ 0.5123, \mathrm{s}_4 = 2.0529$. This solution corresponds to the same values in Figure8.

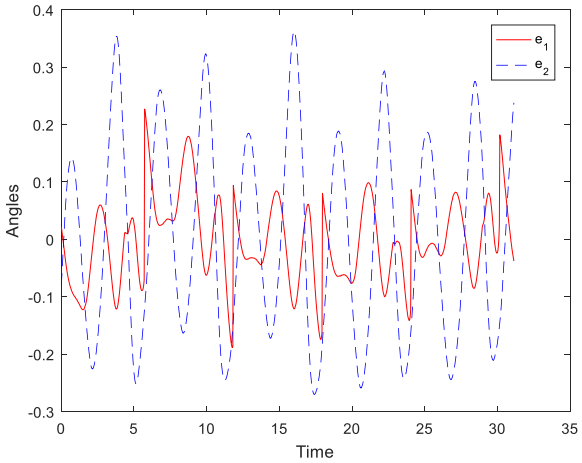

Figure 10 The Error between outputs of CPGs and Real data

Surman Journal for Science and Technology
ISSN: Online (2790-5721) - Print (2790-5713)
sjst.scst.edu.ly
مجلة صرمان للعلوم والتقنية
Vol6, No.2, Jun. – Dec. 2024
Pages: 150 ~ 167

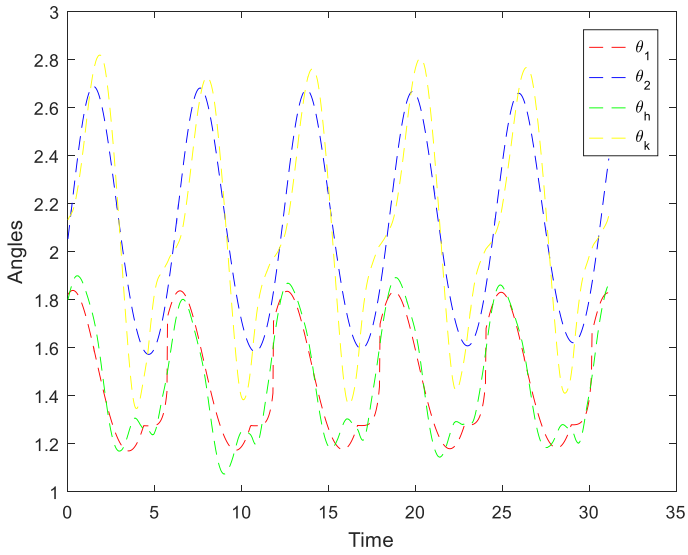

Figure 11: Angles of the real data and output of CPGs.

Tables 3: Uncoupled two neural networks in bounded in 31.13 seconds (N_in_pop=90)

Parameters value $\{\sigma_{s1}, \sigma_{f1}, \tau_{s1}, \tau_{m1}, A_{f1}, I_{inj1}, \sigma_{s2}, \sigma_{f2}, \tau_{s2}, \tau_{m2}, A_{f2}, I_{inj2}, s_1, s_2, s_3, s_4\}$	J	x_b	Cross over
0.2224 1.2321 0.2918 0.0594 12.2561 0.2640 1.2703 0.2073 0.0523 22.7630 0.3914 1.8216 0.5122 2.0533	33.6612	0.8954	0.2
0.2225 1.2323 0.2922 0.0596 12.2547 0.2640 1.2704 0.2074 0.0523 22.7631 0.3919 1.8227 0.5124 2.0540	33.6879	0.8920	0.4
0.2160 1.2249 0.2815 0.0560 12.6823 0.2586 1.2643 0.2000 0.0496 23.6497 0.3778 1.8134 0.5024 2.0523	33.5311	0.8969	0.6
0.2160 1.2249 0.2815 0.0560 12.7106 0.2587 1.2645 0.2001 0.0496 23.6526 0.3786 1.8147 0.5039 2.0571	33.5124	0.9118	0.8
0.2159 1.2248 0.2810 0.0559 12.7139 0.2417 1.2472 0.2023 0.0468 23.6972 0.3780 1.8137 0.4694 2.0530	33.5764	0.8985	1.0

sjst.scst.edu.ly
Surman Journal for Science and Technology
ISSN: Online (2790-5721) - Print (2790-5713)
مجلة صرمان للعلوم والتقنية
Vol6, No.2, Jun. – Dec. 2024
Pages: 150 ~ 167

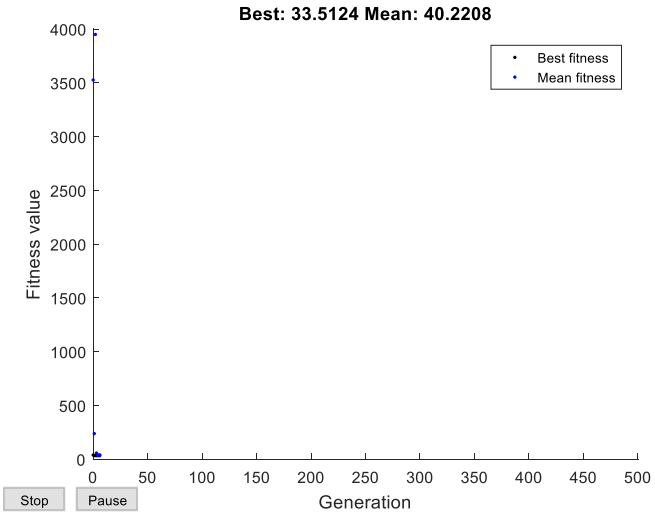

Figure 12: The optimization results are corresponding to the initial conditions $V(0) = 1$ and $q(0) = 1$, with crossover 0.8.

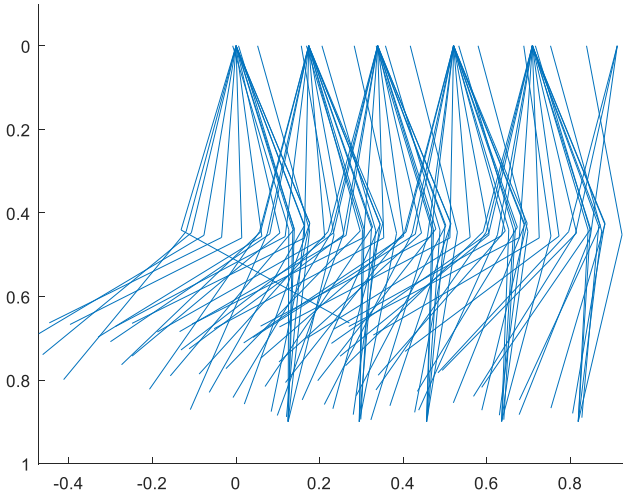

Figure 13 : One leg animation Uncoupled two CPGs: This animation corresponds to the values: $\sigma_{s1} = 0.2160, \sigma_{f1} = 1.2249\ , \tau_{s1} = 0.2815, \tau_{m1} = \ 0.0560,\ A_{f1} = 12.7106,\ \sigma_{s2} = 0.2587,$ $\sigma_{f2} = 1.2645\ ,\quad \tau_{s2} = \ 0.2001,\qquad \tau_{m2} = 0.0496,\quad A_{f2} = 23.6526\ , \mathrm{s}_1 = 0.3786, \mathrm{s}_2 =$ $1.8147\ , \mathrm{s}_3 = \ 0.5039, \mathrm{s}_4 = \ 2.0571,$. This solution corresponds to the same values in Figure12

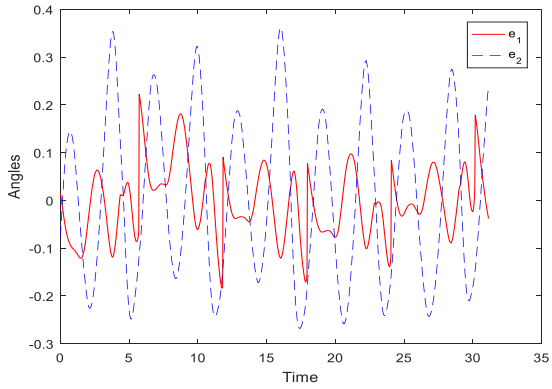

Figure 14 The Error between outputs of CPGs and Real data

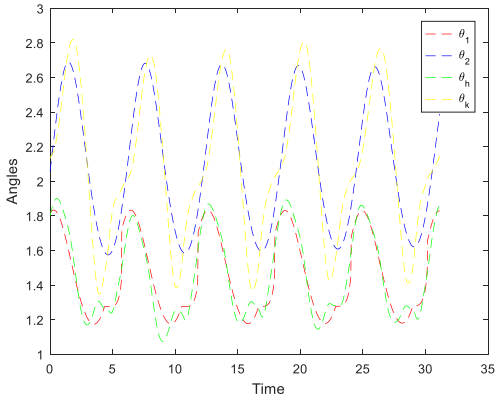

Figure 15: Angles of the real data and output of CPGs.

Tables 4: Uncoupled two neural networks in bounded in 31.13 seconds (N_in_pop=120)

Parameters value $\{\sigma_{s1}, \sigma_{f1}, \tau_{s1}, \tau_{m1}, A_{f1}, I_{inj1}, \sigma_{s2}, \sigma_{f2}, \tau_{s2}, \tau_{m2}, A_{f2}, I_{inj2}, s_1, s_2, s_3, s_4\}$					J	x_b	Cross over
0.2161	1.2250	0.2817	0.0561	12.7103			
0.2588	1.2646	0.2003	0.0497	23.6441	33.5124	0.9118	0.2
0.3788	1.8148	0.5041	2.0570				
0.2162	1.2251	0.2819	0.0561	12.7099			
0.2589	1.2647	0.2003	0.0497	23.6435	33.5249	0.8973	0.4
0.3794	1.8163	0.5043	2.0573				
0.2163	1.2252	0.2814	0.0561	12.7033			
0.2590	1.2648	0.2003	0.0497	23.6418	33.5145	0.9027	0.6
0.3792	1.8167	0.5051	2.0599				
0.2090	1.2169	0.2677	0.0519	13.3852			
0.2421	1.2473	0.1952	0.0454	24.4737	33.4264	0.9159	0.8
0.3654	1.8095	0.4693	2.0475				
0.2085	1.2162	0.2646	0.0513	13.5184			
0.2159	1.2207	0.1973	0.0409	24.7945	33.4966	0.9273	1.0
0.3638	1.8043	0.4175	2.0432				

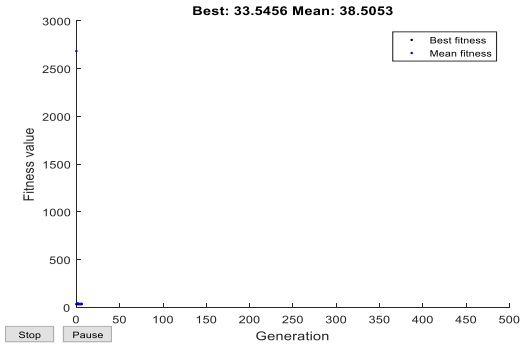

Figure 16: The optimization results are corresponding to the initial conditions $V(0) = 1$ and $q(0) = 1$, with crossover 0.8.

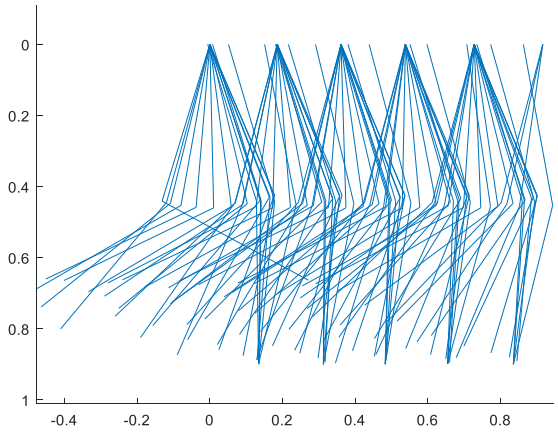

Figure 17 : One leg animation Uncoupled two CPGs: This animation corresponds to the values: $\sigma_{s1} = 0.2090$, $\sigma_{f1} = 1.2169$, $\tau_{s1} = 0.2677$, $\tau_{m1} = 0.0519$, $A_{f1} = 13.3852$, $\sigma_{s2} = 0.2421$, $\sigma_{f2} = 1.2473$, $\tau_{s2} = 0.1952$, $\tau_{m2} = 0.0454$, $A_{f2} = 24.4737$, $s_1 = 0.3654$, $s_2 = 1.8095$, $s_3 = 0.4693$, $s_4 = 2.0475$,. This solution corresponds to the same values in Figure16

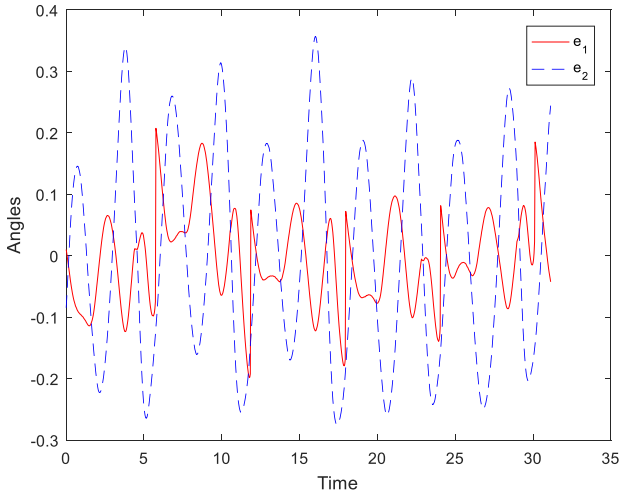

Figure 18: The Error between outputs of CPGs and Real data

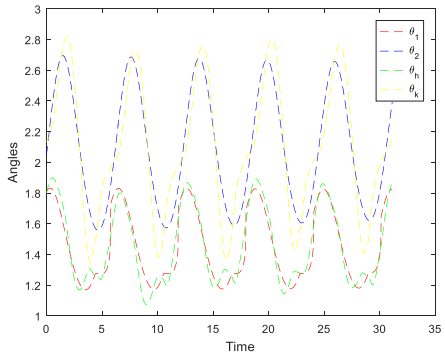

Figure 19: Angles of the real data and output of CPGs.

OPTIMIZATION RESULTS ANALYSIS:

During optimization by using Genetic Algorithm and Hybrid function, also it is used ode23 solve and population size 45, we obtain that the best result when the crossover is 0.8, we get that the objective function is $J = 33.9190$. While in the second trial, we did optimization under population size 6, we obtain that the best result when the crossover is 0.6, we get that the objective function is $J = 33.6471$. The third trial, we did optimization under population size 90, we get that the best result when the crossover is 0.8, we get that the objective function is $J = 33.5124$. Likewise in the fourth trial, we did optimization under population size 120, we obtain that the best result when the crossover is 0.8, we get that the objective function is $J = 33.4264$.

THE STUDY OF PARAMETERS:

In this part of the study, we experimented with optimizing the parameters of Central Pattern Generators (CPGs) to identify the parameters that have the most significant impact on system performance. Our findings reveal that parameters $\sigma_{s_2}, \sigma_{s_3}$ are the most sensitive to changes. Specifically, when the value of either parameter is slightly decreased, the foot begins to oscillate around its starting point. The detailed results are presented in the following table5:

Table5: Compare the optimization of the bidirectional two CPGs with the real data by changing the value of $\sigma_{s_2}, \sigma_{s_3}$.

Changing the value of $\sigma_{s_2}, \sigma_{s_3}$ depends on the results of the optimization in the Figure 17				
Parameters value $\{\sigma_{s1,}\ \sigma_{f1}, \tau_{s1}, \tau_{m1}, A_{f1}, I_{inj1}, \sigma_{s2,}\ \sigma_{f2}, \tau_{s2}, \tau_{m2}, A_{f2}, I_{inj2}\ , s_1, s_2, s_3, s_4\}$	σ_{s_2}	σ_{s_3}	J	x_b
0.2090 1.2169 0.2677 0.0519 13.3852 0.2421 1.2473 0.1952 0.0454 24.4737 0.3654 1.8095 0.4693 2.0475	0.2090	0.2421	33.4264	0.9159
0.2080 1.2169 0.2677 0.0519 13.3852 0.2410 1.2473 0.1952 0.0454 24.4737 0.3654 1.8095 0.4693 2.0475	0.2080	0.2410	33.4264	0.8727

Likewise, making a small reduction in the constant values $\sigma_{f_2}, \sigma_{f_3}$ causes a normal foot movement in the initial phases, but the movement soon shifts to an abnormal state. Table6 provides a summary of the results obtained from this reduction:

Table6: Compare the optimization of the bidirectional two CPGs with the real data by changing the value of $\sigma_{f_2}, \sigma_{f_3}$.

Changing the value of $\sigma_{f_2}, \sigma_{f_3}$ depends on the results of the optimization in the Figure 17								
Parameters value $\{\sigma_{s1,}\ \sigma_{f1}, \tau_{s1}, \tau_{m1}, A_{f1}, I_{inj1}, \sigma_{s2,}\ \sigma_{f2}, \tau_{s2}, \tau_{m2}, A_{f2}, I_{inj2}, s_1, s_2, s_3, s_4\}$					σ_{f_2}	σ_{f_3}	J	x_b
0.2090	1.2169	0.2677	0.0519	13.3852	1.2169	1.2473		
0.2421	1.2473	0.1952	0.0454	24.4737			33.4264	0.9159
0.3654	1.8095	0.4693	2.0475					
0.2090	1.2130	0.2677	0.0519	13.3852	1.2130	1.2463		
0.2421	1.2463	0.1952	0.0454	24.4737			33.4264	0
0.3654	1.8095	0.4693	2.0475					

Similarly, when the values of τ_{s_2}, τ_{s_3} are slightly decreased, both displacement and velocity decrease, and while the foot movement was initially normal, it began to oscillate. The table7 illustrates this result:

Table7: Compare the optimization of the bidirectional two CPGs with the real data by changing the value of τ_{s_2}, τ_{s_3}.

Changing the value of τ_{s_2}, τ_{s_3} depends on the results of the optimization in the Figure 17								
Parameters value $\{\sigma_{s1,}\ \sigma_{f1}, \tau_{s1}, \tau_{m1}, A_{f1}, I_{inj1}, \sigma_{s2,}\ \sigma_{f2}, \tau_{s2}, \tau_{m2}, A_{f2}, I_{inj2}, s_1, s_2, s_3, s_4\}$					τ_{s_2}	τ_{s_3}	J	x_b
0.2090	1.2169	0.2677	0.0519	13.3852	0.2677	0.1952		
0.2421	1.2473	0.1952	0.0454	24.4737			33.4264	0.9159
0.3654	1.8095	0.4693	2.0475					
0.2090	1.2169	0.2667	0.0519	13.3852	0.2667	0.1942		
0.2421	1.2473	0.1942	0.0454	24.4737			33.4264	-0.6906
0.3654	1.8095	0.4693	2.0475					

Likewise, a small reduction in the constant values c and v results in an initial forward movement of the foot, followed by a backward retraction, ultimately leading to an abnormal gait. The following table summarizes these findings :

Table8: Compare the optimization of the bidirectional two CPGs with the real data by changing the value of τ_{m_2}, τ_{m_3}.

Changing the value of τ_{m_2}, τ_{m_3} depends on the results of the optimization in the Figure 17								
Parameters value $\{\sigma_{s1,}\ \sigma_{f1}, \tau_{s1}, \tau_{m1}, A_{f1}, I_{inj1}, \sigma_{s2,}\ \sigma_{f2}, \tau_{s2}, \tau_{m2}, A_{f2}, I_{inj2}, s_1, s_2, s_3, s_4\}$					τ_{m_2}	τ_{m_3}	J	x_b

0.2090 1.2169 0.2677 0.0519 13.3852 0.2421 1.2473 0.1952 0.0454 24.4737 0.3654 1.8095 0.4693 2.0475	0.0519	0.0454	33.4264	0.9159
0.2090 1.2169 0.2677 0.0510 13.3852 0.2421 1.2473 0.1952 0.0444 24.4737 0.3654 1.8095 0.4693 2.0475	0.0510	0.0444	33.4264	0.4798

Likewise, a small reduction in the constant values A_{f_2}, A_{f_3} results in a backward movement of the foot, maintaining the same displacement and velocity. This finding is summarized in Table9:

Table9: Compare the optimization of the bidirectional two CPGs with the real data by changing the value of A_{f_2}, A_{f_3}.

Changing the value of A_{f_2}, A_{f_3} depends on the results of the optimization in the Figure 17				
Parameters value $\{\sigma_{s1}, \sigma_{f1}, \tau_{s1}, \tau_{m1}, A_{f1}, I_{inj1}, \sigma_{s2}, \sigma_{f2}, \tau_{s2}, \tau_{m2}, A_{f2}, I_{inj2}, s_1, s_2, s_3, s_4\}$	A_{f_2}	A_{f_3}	J	x_b
0.2090 1.2169 0.2677 0.0519 13.3852 0.2421 1.2473 0.1952 0.0454 24.4737 0.3654 1.8095 0.4693 2.0475	13.3852	24.4737	33.4264	0.9159
0.2090 1.2169 0.2677 0.0519 15.3852 0.2421 1.2473 0.1952 0.0454 25.4737 0.3654 1.8095 0.4693 2.0475	15.3852	25.4737	33.4264	0.0138

CONCLUSION:

The Rothstein-Silverstein neural model was employed to identify human walking patterns using a genetic algorithm and a hybrid function. The study revealed that when comparing the neural model's results to real-world data, the injected current 'c' had to be removed as it introduced errors that hindered the comparison. This led to a transformation of the model from a neural model to a central pattern generator (CPG). Real-world data was obtained using the Tema Motion software. Additionally, experiments showed that slight alterations in the parameter settings of the Rothstein-Silverstein model resulted in varying outcomes.

REFERENCE:

1. Abdalftah, E. and A. Elbori, *Optimizing and Analyzing the stability of The Rowat-Selverston Neural Oscillator for One-Legged Locomotion.* Int. J. Adv. Res. Sci. Technol. Volume, 2023. **12**(11): p. 1174-1181.
2. Elbori, A. and A. Ellafi, *Optimization of Coupled harmonic oscillators for Defining One leg Locomotion.*
3. Larsen, J.C., *Central Pattern Generators in modern Science.*
4. Ijspeert, A.J., *Central pattern generators for locomotion control in animals and robots: a review.* Neural Networks, 2008. **21**(4): p. 642-653.
5. Yu, J., et al., *A survey on CPG-inspired control models and system implementation.* IEEE Transactions on neural networks and learning systems, 2014. **25**(3): p. 441-456.

6. Billard, A. and A.J. Ijspeert. *Biologically inspired neural controllers for motor control in a quadruped robot*. in *Neural Networks, 2000. IJCNN 2000, Proceedings of the IEEE-INNS-ENNS International Joint Conference on*. 2000. IEEE.
7. Bucher, D., et al., *Central pattern generators.* eLS, 2000.
8. Casasnovas, B. and P. Meyrand, *Functional differentiation of adult neural circuits from a single embryonic network.* The Journal of neuroscience, 1995. **15**(8): p. 5703-5718.
9. Van Vreeswijk, C., L. Abbott, and G.B. Ermentrout, *When inhibition not excitation synchronizes neural firing.* Journal of computational neuroscience, 1994. **1**(4): p. 313-321.
10. Arikan, K.B. and B. Irfanoglu, *A Test Bench to Study Bioinspired Control for Robot Walking.* Journal of Control Engineering and Applied Informatics, 2011. **13**(2): p. 76-80.
11. Elbori, A.E.G., M. Turan, and K.B. Arıkan, *Optimization of Central Patterns Generators.* 2017.
12. Jiaqi, Z., et al., *Dynamic walking of AIBO with Hopf oscillators.* Chinese Journal of Mechanical Engineering, 2011. **24**(4): p. 612-617.
13. Marbach, D., *Evolution and Online Optimization of Central Pattern Generators for Modular Robot Locomotion.* Unpublished Master Thesis, Swiss Federal Institute of Technology Lausanne, 2004.
14. Williamson, M.M., *Robot arm control exploiting natural dynamics*. 1999, Massachusetts Institute of Technology.
15. Taga, G., Y. Yamaguchi, and H. Shimizu, *Self-organized control of bipedal locomotion by neural oscillators in unpredictable environment.* Biological cybernetics, 1991. **65**(3): p. 147-159.
16. Taga, G., *A model of the neuro-musculo-skeletal system for anticipatory adjustment of human locomotion during obstacle avoidance.* Biological Cybernetics, 1998. **78**(1): p. 9-17.
17. Aoi, S. and K. Tsuchiya, *Locomotion control of a biped robot using nonlinear oscillators.* Autonomous robots, 2005. **19**(3): p. 219-232.
18. Endo, G., et al. *Experimental studies of a neural oscillator for biped locomotion with QRIO*. in *Proceedings of the 2005 IEEE international conference on robotics and automation*. 2005. IEEE.
19. Torres-Huitzil, C. and B. Girau. *Implementation of central pattern generator in an FPGA-based embedded system*. in *International Conference on Artificial Neural Networks*. 2008. Springer.
20. Golden, J., *Gait synthesis for the SD-2 biped robot to climb stairs.* International Journal of Robotics & Automation, 1990. **5**(4): p. 149-159.
21. Kajita, S. and K. Tani. *Study of dynamic biped locomotion on rugged terrain-theory and basic experiment*. in *Advanced Robotics, 1991.'Robots in Unstructured Environments', 91 ICAR., Fifth International Conference on*. 1991. IEEE.